Electronic Supporting Information (ESI)

Fabricating penta-coordinated Fe single atom for electrochemical CO_2 reduction to syngas

Linjie Wang,‡[a] Xiaofei Lai,‡[b] Yafeng Xu,‡[c] Shaojuan Luo,*[a,d,e] Lu Wang,*[c] Kai Yan,[d] Da Zhang, [a] Sitong Feng[a] and Yong Xu*[b]

[a]School of Chemical Engineering and Light Industry, Guangdong University of Technology, Guangzhou 510006, China.

[b]Guangzhou Key Laboratory of Low-Dimensional Materials and Energy Storage Devices, Collaborative Innovation Center of Advanced Energy Materials, School of Materials and Energy, Guangdong University of Technology, Guangzhou 510006, China.

[c]Institute of Functional Nano & Soft Materials (FUNSOM), Jiangsu Key Laboratory for Carbon-Based Functional Materials & Devices, Soochow University, Suzhou, 215123, China.

[d]Guangdong Provincial Key Laboratory of Environmental Pollution Control and Remediation Technology, Sun Yat-Sen University, Guangzhou 510006, China.

[e]Jieyang Branch of Chemistry and Chemical Engineering Guangdong Laboratory, Rongjiang Laboratory, Jieyang, 515200, China.

*Corresponding author kesjluo@gdut.edu.cn, lwang22@suda.edu.cn, yongxu@gdut.edu.cn

Computational methods

DFT calculations were performed by the Vienna ab initio simulation package (VASP).[1, 2] The ion-electron interaction was described by the projector augmented wave (PAW) method,[3] while the generalized gradient approach (GGA) of the Perdew-Burke-Ernzerhof (PBE) functional[4, 5] was employed to account for the electron-electron exchange correlation. Furthermore, the van der Waals interaction was also considered in this study by using DFT-D_3 correction.[6] The cutoff energy for the plane wave basis sets was defined as 500 eV. The geometry optimization was converged if the maximum force on each atom reached 0.03 eV $Å^{-1}$. For Fe−N_5/C and Fe NP/NC structures, a 6×6 supercell of graphene was constructed by missing two adjacent C atoms, and four C atoms in the defective site were replaced by four N atoms. The structures were relaxed using a k-point mesh of 3×3×1 generated by Gamma centered grid. A vacuum space of 15 Å was introduced to avoid the interaction between periodic images. The Gibbs free energy changes (ΔG) were calculated by the following formula (Table S4).[7]

$$\Delta G = \Delta E + \Delta ZPE - T\Delta S$$

where ΔE describes the adsorption energy, ΔZPE and ΔS are the correction of zero-point energy and entropy for the adsorbed intermediates, T is the temperature (298.15 K).

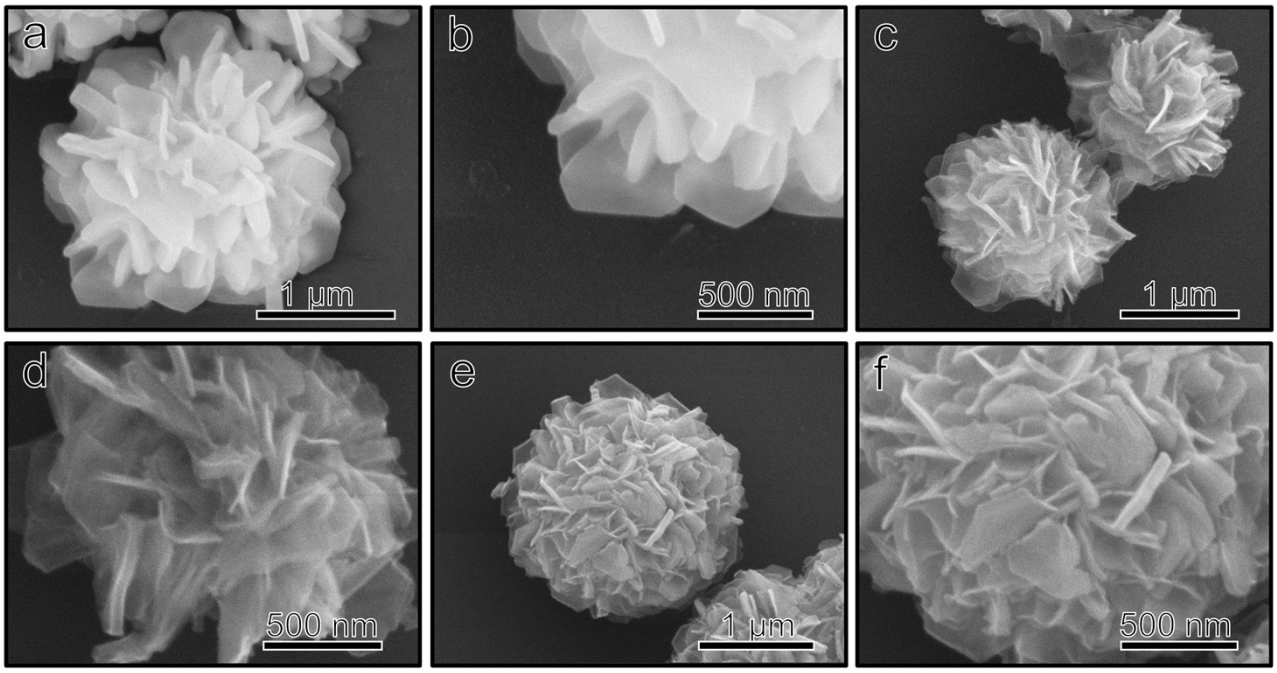

Figure S1. SEM images of (a, b) ZTF, (c, d) NC, and (e, f) Fe–N_5/C.

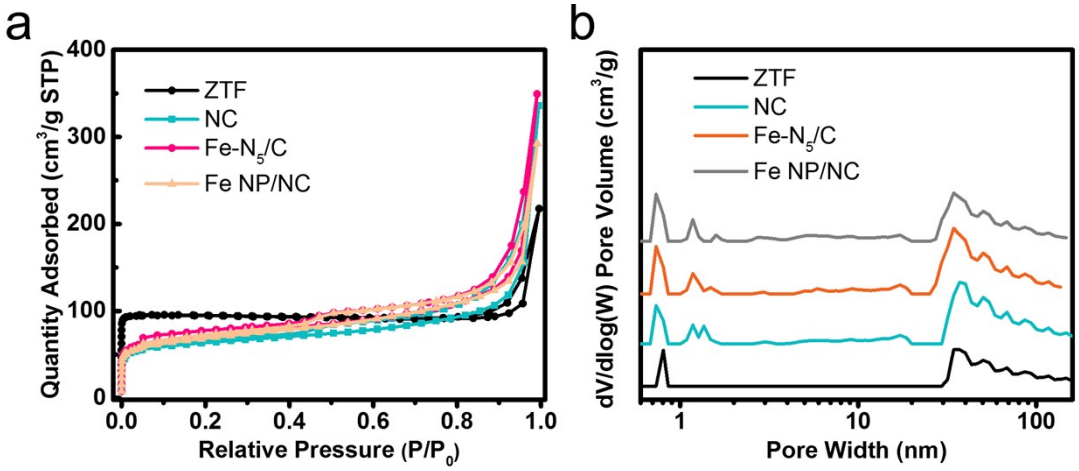

Figure S2. (a) N_2 adsorption-desorption isotherms of ZIF, NC, Fe–N_5/C, and Fe NP/NC; (b) pore structures of ZIF, NC, Fe–N_5/C, and Fe NP/NC.

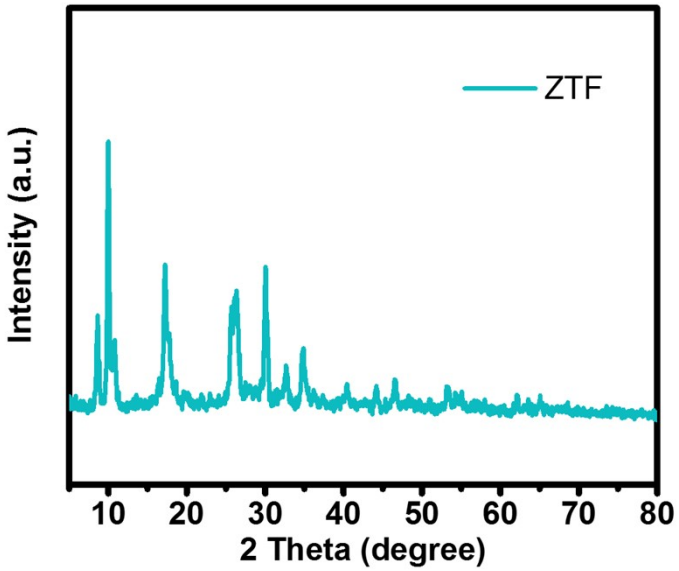

Figure S3. XRD pattern of ZTF.

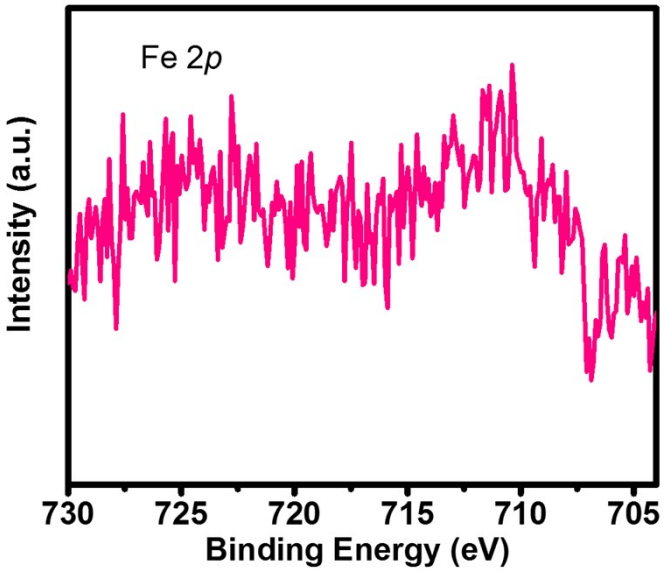

Figure S4. High-resolution XPS spectrum of the Fe 2*p* of Fe–N_5/C.

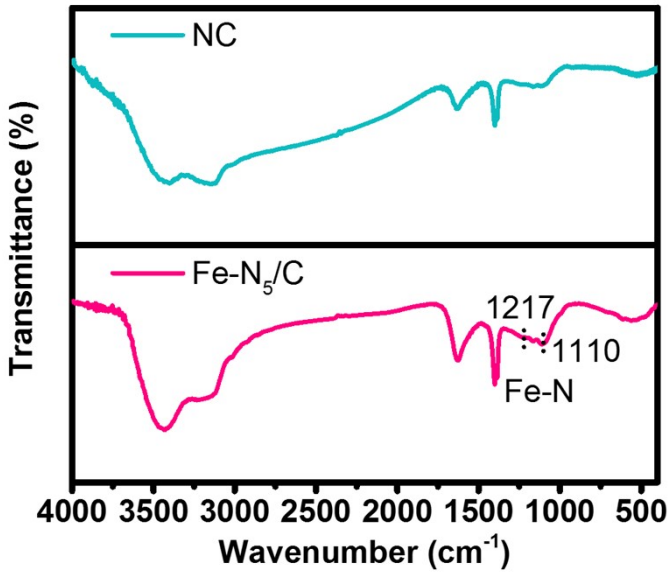

Figure S5. FT-IR spectra of NC and Fe–N_5/C.

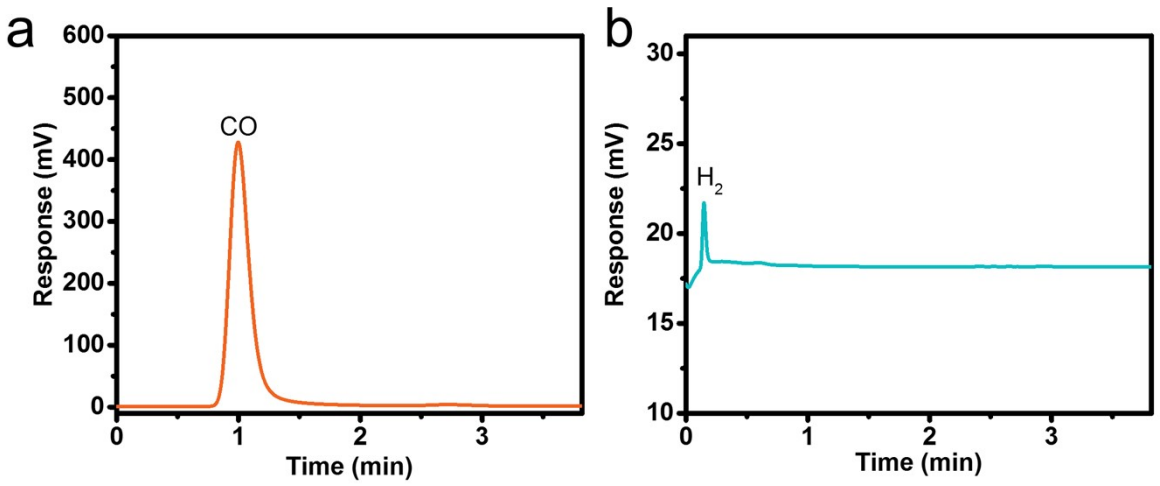

Figure S6. Representative spectra of (a) flame ionization detector (FID) and (b) thermal conductivity discharge detector (TCD) taken for the Fe-N_5/C at −0.7 V.

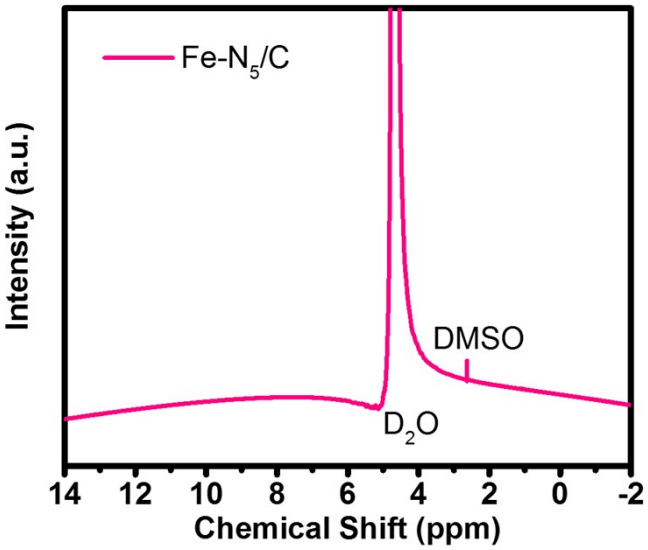

Figure S7. ^{1}H NMR spectrum of the liquid product obtained over Fe–N_5/C after 1 h CO_2 reduction at −0.7 V.

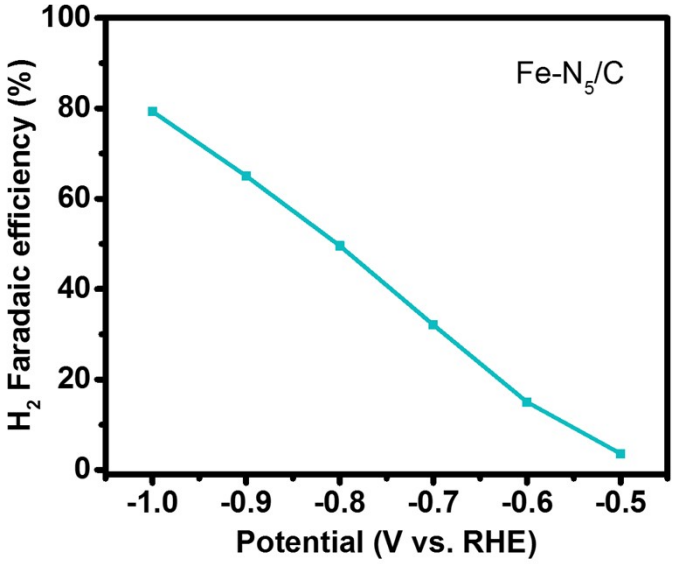

Figure S8. Faradic efficiencies of H_2 for the Fe−N_5/C at various applied potentials.

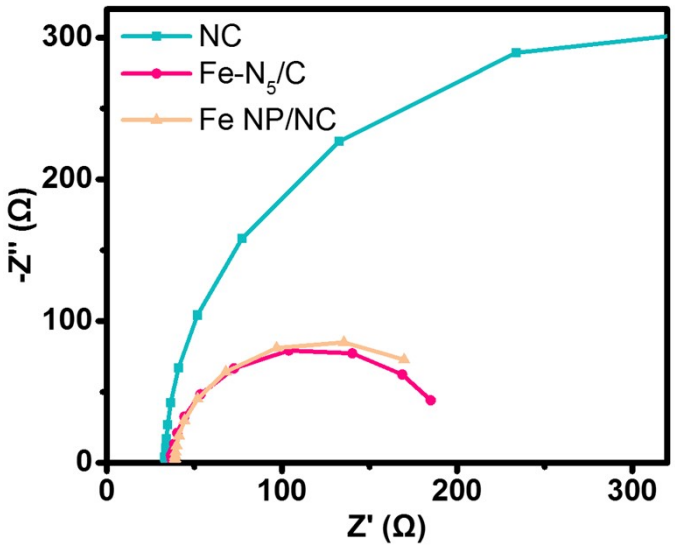

Figure S9. EIS Nyquist plots of NC, Fe–N_5/C, and Fe NP/NC.

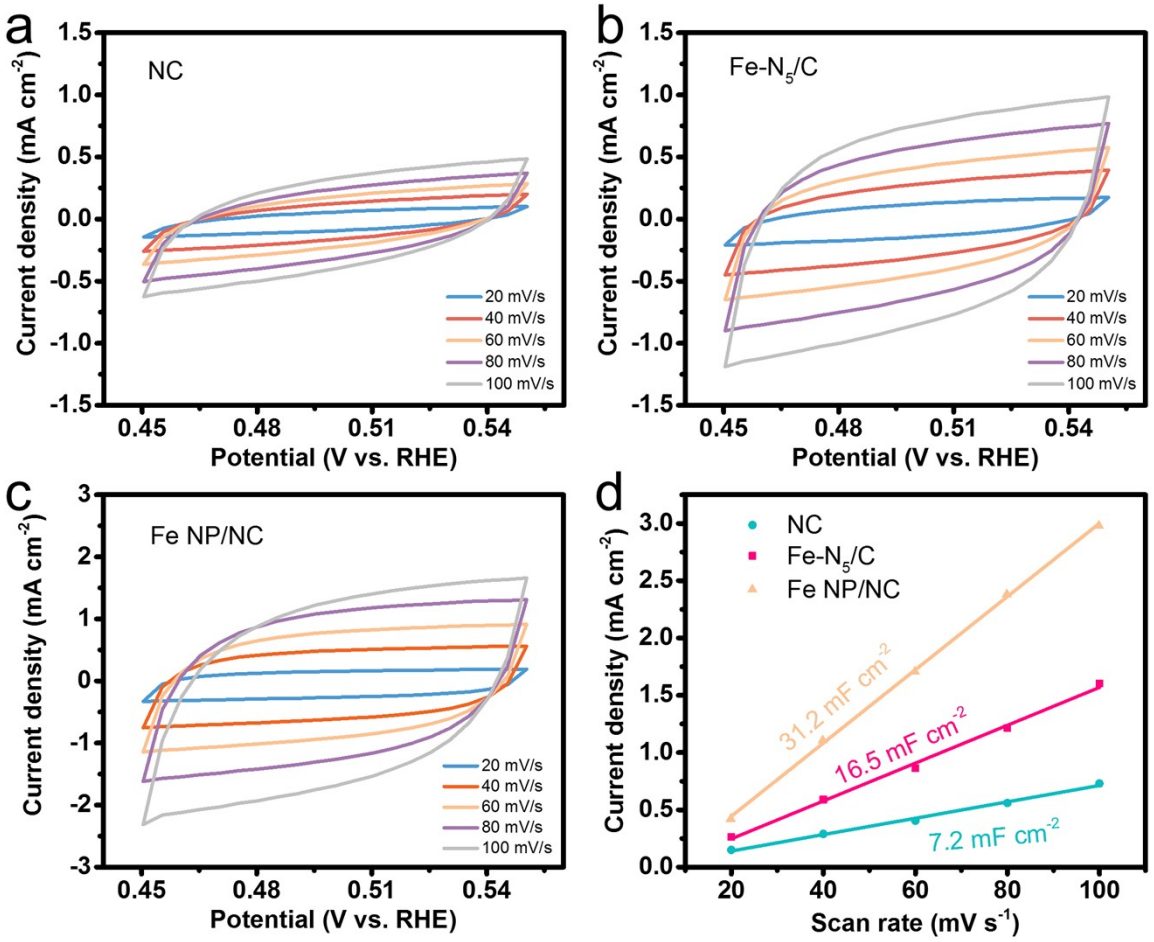

Figure S10. Cyclic voltammograms of (a) NC, (b) Fe–N_5/C, and (c) Fe NP/NC at different scan rates (20, 40, 60, 80, and 100 mV·s^{-1}). (d) Double layer capacitive currents plotted against scan rates performed in CO_2-saturated 1.0 M KOH solution.

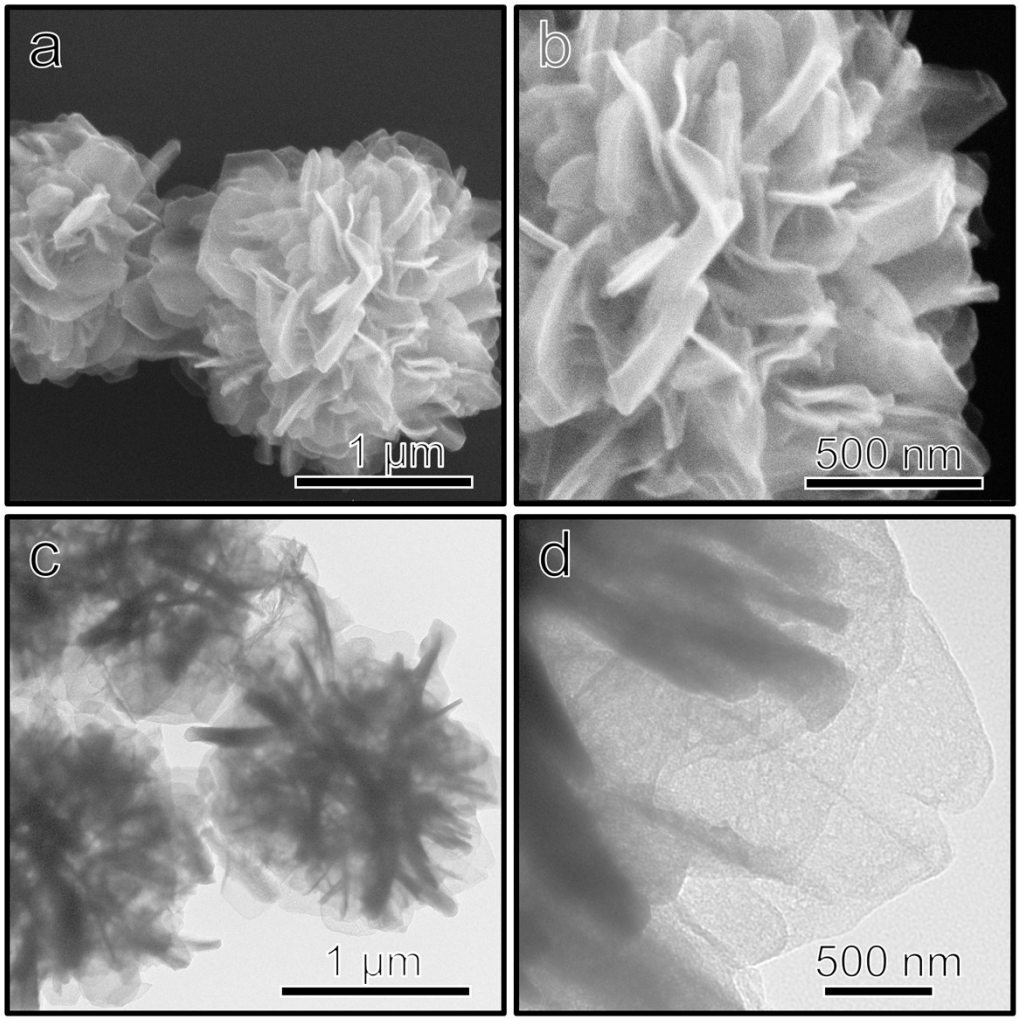

Figure S11. (a, b) SEM and (c, d) TEM images of the used Fe–N_5/C.

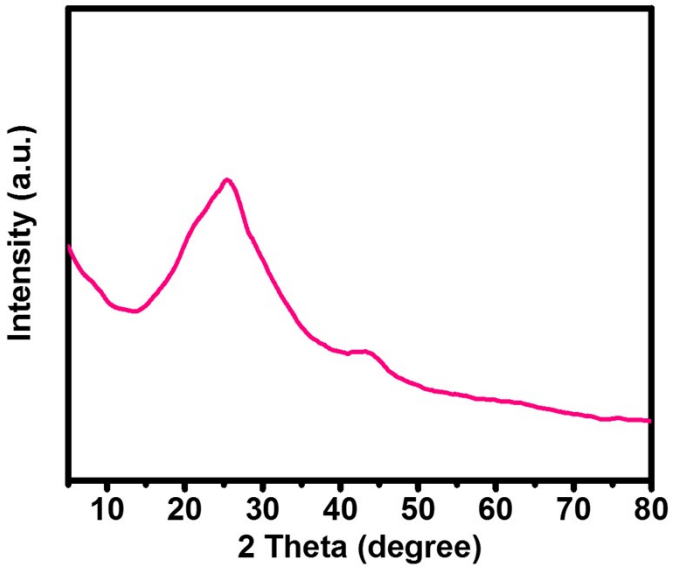

Figure S12. XRD pattern of Fe–N_5/C after 12 h electrolysis.

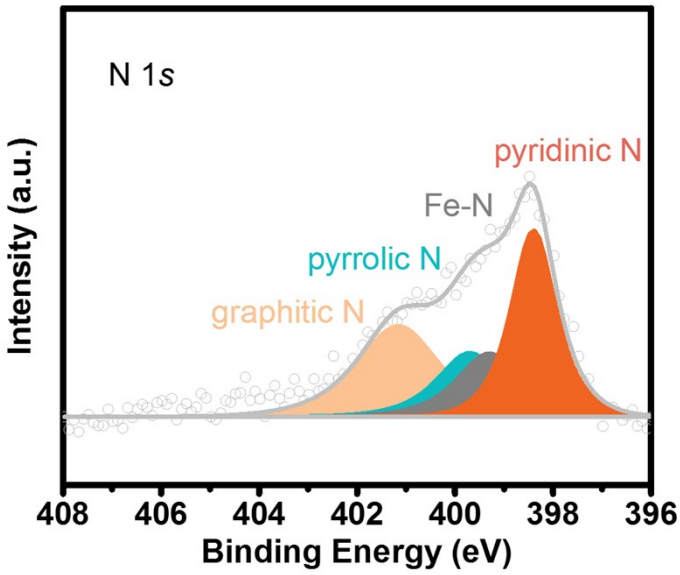

Figure S13. N 1s XPS spectra of Fe–N_5/C after 12 h electrolysis.

Table S1. BET analysis results of samples.

Catalysts	S_{BET} (m^2/g)[a]	V_{meso} (cm^3/g)[b]	V_{micro} (cm^3/g)[c]
ZTF	288.2	~	0.145
NC	200.8	0.457	0.056
Fe–N_5/C	235.1	0.464	0.058
Fe NP/NC	226.0	0.391	0.048

[a]: S_{BET} is BET specific surface area.

[b]: V_{meso} is the specific mesopore volume calculated from desorption isotherm by the BJH method.

[c]: V_{micro} is the specific micropore volume calculated by the *t*-plot method.

Table S2. EXAFS fitting results of Fe−N_5/C.

Scattering Paths	CN[a]	R (Å)[b]	σ^2 (10^{-3} Å^2)[c]	ΔE_o (eV)[d]
Fe−N	5.15 ± 1.21	1.98 ± 0.1	7.00 ± 0.01	-6.51 ± 6.06

[a]: Coordination number.

[b]: Interatomic distance.

[c]: Debye-Waller factor.

[d]: Energy deviation.

Table S3. Comparison between Fe−N_5/C and other reported catalysts for CO_2RR.

Catalysts	Electrolyte	maximum FE_{CO} (%)	J_{CO} (mA cm^{-2})	H_2/CO	Reference
Fe−N_5/C	0.1 M $KHCO_3$	67.8	3.8	0.15/1~2.8/1	This work
Pd/C	0.5 M $NaHCO_3$	40	1	2/1~1/1	[8]
Pd/TaC	0.5 M $NaHCO_3$	45	0.5	6/1~1/1	[9]
Pd/NMs	0.5 M KOH	48	2.5	2/1~1/1	[10]
Ag NCs	0.1 M $KHCO_3$	55	2	2/1~1/1	[11]
Cu nanowire arrays	0.1 M $KHCO_3$	40	2	3/1~1/2	[12]
Cu_{ZIF}-T	~	40	2	3/1~1/2	[13]
N-doped carbon	0.1 M $KHCO_3$	65	2	3/1~1/2	[14]
CuInO/C	0.1 M $KHCO_3$	42	~	~0.83	[15]
Pd/NbN	0.5 M $NaHCO_3$	38.4	0.4	1.35/1~6.25/1	[16]
CuO-400	0.1 M $KHCO_3$	48.2	1.4	1/1~2/1	[17]
Pd@CuO-2	0.5 M $NaHCO_3$	58.3	2.2	0.44/1~0.72/1	[18]
Co@CoNC-900	0.1 M $KHCO_3$	42	3.2	1/1~1.5/1	[19]
Col-Au	0.5 M $KHCO_3$	35	1	1.8/1~2.2/1	[20]
F-Cu_2O	0.1 M $KHCO_3$	53.2	0.9	0.5/1~1/1	[21]
Bulk In	0.1 M $KHCO_3$	38	0.2	0.2/1~1/1	[22]
Cu/In_2O_3 NPs/C-H_2	0.1 M $KHCO_3$	31.1	2.1	1.6/1~2/1	[23]

Table S4. Free energies of molecule species.[a]

Species	*E* (eV)	ZPE (eV)	TS (eV)
H_2 (g)	−6.77	0.27	0.41
H_2O (l)	−14.22	0.56	0.67
CO (g)	−15.28	0.14	0.61
CO_2 (g)	−22.96	0.31	0.66

[a]: A −0.51 eV correction to energy of CO (g) is included due to the use of PBE functional.

References

1. G. Kresse and J. Furthmüller, *Comput. Mater. Sci.* , 1996, **6**, 15-50.
2. G. Kresse and J. Furthmüller, *Phys. Rev. B*, 1996, **54**, 11169-11186.
3. P. E. Blöchl, *Phys. Rev. B*, 1994, **50**, 17953-17979.
4. J. P. Perdew, M. Ernzerhof and K. Burke, *J. Chem. Phys.*, 1996, **105**, 9982-9985.
5. J. P. Perdew, K. Burke and M. Ernzerhof, *Phys. Rev. Lett.* , 1996, **77**, 3865-3868.
6. S. Grimme, J. Antony, S. Ehrlich and H. Krieg, *J. Chem. Phys.*, 2010, **132**, 154104-154122.
7. J. K. Nørskov, J. Rossmeisl, A. Logadottir, L. Lindqvist, J. R. Kitchin, T. Bligaard and H. Jonsson, *The Journal of Physical Chemistry B*, 2004, **108**, 17886-17892.
8. W. Sheng, S. Kattel, S. Yao, B. Yan, Z. Liang, C. J. Hawxhurst, Q. Wu and J. G. Chen, *Energy Environ. Sci.* , 2017, **10**, 1180-1185.
9. J. Wang, S. Kattel, C. J. Hawxhurst, J. H. Lee, B. M. Tackett, K. Chang, N. Rui, C. J. Liu and J. G. Chen, *Angew. Chem. Int. Ed.*, 2019, **58**, 6271-6275.
10. J. Wu, Y. Xie, Z. Ren, S. Du, H. Meng, L. Zhao, X. Wang, G. Wang and H. Fu, *ChemSusChem*, 2019, **12**, 3304-3311.
11. X. Han, L. Liu, J. Yuan, X. Zhang and D. Niu, *ChemSusChem*, 2021, **14**, 721-729.
12. R. Daiyan, R. Chen, P. Kumar, N. M. Bedford, J. Qu, J. M. Cairney, X. Lu and R. Amal, *ACS Appl. Mater. Interfaces*, 2020, **12**, 9307-9315.
13. S. Cui, C. Yu, X. Tan, H. Huang, X. Yao and J. Qiu, *ACS Sustain. Chem. Eng.*, 2020, **8**, 3328-3335.
14. H. Li, N. Xiao, Y. Wang, C. Li, X. Ye, Z. Guo, X. Pan, C. Liu, J. Bai and J. Xiao, *J. Mater. Chem. A*, 2019, **7**, 18852-18860.
15. C. Shen, P. Wang, L. Li, X. Huang and Q. Shao, *Nano Res.*, 2022, **15**, 528-534.
16. Y. Liu, D. Tian, A. N. Biswas, Z. Xie, S. Hwang, J. H. Lee, H. Meng and J. G. Chen, *Angew. Chem. Int. Ed.*, 2020, **59**, 11345-11348.
17. X. Yao, Y. Guo, B. Liu, P. Wang, J. Sun, W. Li and C. Zhao, *ChemElectroChem*, 2021, **8**, 592-602.
18. R. Cai, X. Du, G. Liu, X. Wang, Q. Tang, X. Pan, F. Li and J. Li, *Fuel*, 2023, **338**, 127346-127353.

19. Y. Wang, C. Niu, Y. Zhu, D. He and W. Huang, *ACS Appl. Energ. Mater.*, 2020, **3**, 9841-9847.
20. L. Mascaretti, A. Niorettini, B. R. Bricchi, M. Ghidelli, A. Naldoni, S. Caramori, A. Li Bassi and S. Berardi, *ACS Appl. Energ. Mater.*, 2020, **3**, 4658-4668.
21. H. Luo, B. Li, J. G. Ma and P. Cheng, *Angew. Chem. Int. Ed.*, 2022, **134**, e202116736.
22. S. A. Mahyoub, F. A. Qaraah, S. Yan, A. Hezam, C. Chen, J. Zhong and Z. Cheng, *J. CO2 Util.*, 2022, **61**, 102033-102044.
23. J. Shen, L. Wang, X. He, S. Wang, J. Chen, J. Wang and H. Jin, *ChemSusChem*, 2022, **15**, e202201350.